"Gheorghe Asachi" Technical University of Iasi, Romania

ELECTROCHEMICAL DECOLORIZATION OF DISPERSE BLUE-1 DYE IN AQUEOUS SOLUTION

Kanayo Oguzie[1,2*], Emeka Oguzie[1], Simeon Nwanonenyi[1], Johnkennedy Edoziem[1], Ladislav Vrsalović[3]

[1]*Africa Centre of Excellence in Future Energies and Electrochemical Systems (ACE-FUELS), Federal University of Technology Owerri, PMB 1526, Owerri, Imo State, Nigeria*
[2]*Department of Environmental Management, Federal University of Technology Owerri, PMB 1526, Owerri, Imo State, Nigeria*
[3]*Faculty of Chemistry and Technology, Department of Electrochemistry and Materials Protection, University of Split, Ruđera Boškovića 35, 21000 Split, Croatia*

Abstract

An electrochemical oxidation procedure using graphite electrodes was employed for decolorizing Disperse Blue-1 dye in aqueous solution, with NaCl as supporting electrolyte. The effects of various factors such as electrolysis time, initial dye concentration, pH, temperature, current density and supporting electrolyte on the dye removal process were studied. Decolorization efficiency increased steadily with electrolysis time, current density and electrolyte concentration, but decreased with increasing dye concentration, while showing a nonlinear trend with pH, with maximum efficiency of 90% obtained at pH 7. Increasing the system temperature from 28 to 50 ºC caused decolorization efficiency to increase, especially at low dye concentration, reaching 96% at 25 mg/L. Decolorization efficiency was subdued at high dye concentrations, even with high current densities. This effect was however overcome by increasing the supporting electrolyte concentration. Density functional theory-based quantum chemical computations showed the amine functions in the p-phenyldiamine moieties to be the reactive sites for oxidative decolorization of disperse blue 1 dye. In summary, electrochemical oxidation using graphite electrodes effectively decolorized Disperse Blue-1 dye in aqueous solution.

Key words: decolorization, density functional theory, electrochemical treatment, Fukui indices
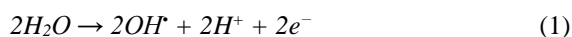
1. Introduction

Dyes are generally used in the food, pharmaceutical, pulp, paper, cosmetic, textile and leather manufacturing industries . The textile industry produces large volumes of wastewater in its dyeing and finishing processes (El-Ashtoukhy et al., 2016; Lopes et al., 2004). Such dye-containing effluents pose considerable environmental concerns, having pronounced impact on natural water bodies, land as well as aquatic organisms (Baddouh et al., 2018; Khalik et al., 2018; Rahimi et al., 2019;). Dyes can be removed from wastewaters by means of biological, physical, or chemical treatment methods (Abd El-Kader et al., 2019; El-Ashtoukhy et al., 2016; Eren et al., 2020; Jan et al., 2020; Kolekar et al., 2008; Pearce et al., 2003; Rahimi et al., 2019). Techniques for removal of synthetic dyes from wastewaters were earlier reviewed by Forgacs et al. (2004) and more recently a critical review of dye decolorization methodologies has been undertaken by Gupta et al. (2015). Most dyes are non-biodegradable due to their complex molecular structures and large sizes and therefore cannot be easily degraded by conventional treatment methods (flocculation, reverse osmosis, precipitation, air stripping, ultra-filtration and adsorption) (An et al., 2012; Kaur and Kaur., 2016; Stergiopoulos et al., 2014). Recently, electrochemical

---

*Author to whom all correspondence should be addressed: e-mail: kanayo.oguzie@futo.edu.ng; Phone: +234 8037069183

treatments have become increasingly useful in the dyes wastewater treatment with promising results (Alves et al., 2013; Awad and Galwa, 2005; Basha et al., 2012; Gholami et al., 2018; El-Sayed et al., 2014; Kariyajjanavar et al., 2011; Koparal et al., 2007).

Electrochemical treatment of dye-containing wastewater is achieved by either direct or indirect electrolysis at the anode, depending on the nature of the electrode materials. Direct electrolysis involves oxidation on the surface of anodes with high electro-catalytic activity, usually by the adsorbed hydroxyl radicals (Eq. 1) and parameters such as current density and diffusion rates of species are key determinants (Jawad and Najim, 2018). Indirect electrolysis involves surface mediators on the anode surface, like chloride salts, added to enhance conductivity as well as generate highly oxidizing hypochlorite ions (OCl^-) from hypochlorous acid (HOCl) as shown in Eq. (2)-(4) (Yong et al., 2011). The generated hypochlorite ions act as the main oxidizing agent in the pollutant decolorization.

$$2H_2O \rightarrow 2OH^\cdot + 2H^+ + 2e^- \qquad (1)$$

$$2Cl^- \rightarrow Cl_2 + 2e^- \qquad (2)$$

$$Cl_2 + H_2O \rightarrow H^+ + HOCl \qquad (3)$$

$$HOCl \rightarrow H^+ + OCl^- \qquad (4)$$

Anthraquinone dyes are an important class of dyes, though with lower tinctorial strengths and complex syntheses routes compared to azo dyes. Their complex structures make their degradation more challenging; hence they pose a serious environmental risk (Routoula and Patwardhan, 2020). Existing experimental reports on the decolorization mechanisms of some anthraquinone dyes suggest different initiation mechanisms for different molecular structures. Zeng et al. (2009) reported that decolorization of disperse blue 56 by a combination of ultraviolet radiation and sodium hypochlorite is initiated by SN_2 nucleophilic reaction involving one of the quinonoid carbonyl groups. Pan et al. (2017) suggested that decolorization of disperse blue 2BLN by *Aspergillus* species proceeds via rupture of C-C bonds of the anthraquinone chromophore at different positions and identified two competing decolorization pathways. Disperse blue 1 (DBD; $C_{14}H_{12}N_4O_2$ - 1,4,5,8-tetraaminoanthracene-9,10-dione) is an aminoanthraquinone dye, used mainly in colour formulations for hair, textiles and plastics, as well as for dying fabrics. It is an eye and skin irritant, with possible mutagenic and carcinogenic effects (Rahimi et al., 2020).

The decolorization of disperse blue 1 dye in aqueous solutions has however not been extensively reported in the literature, hence the decolorization mechanism is still not clear. Saquib et al. (2008) investigated the photocatalytic decolorization of disperse blue 1 using a $UV/TiO_2/H_2O_2$ system. Though their study did not ascertain decolorization

mechanisms, their results highlighted the importance of optimizing decolorization parameters to attain high decolorization efficiencies.

The first step in elucidating the mechanisms of oxidative decolorization of DBD is to accurately ascertain the sites that are most susceptible to attack of the oxidizing agents. A practical route to achieve this, at least at the molecular level, involves density functional theory (DFT)-based quantum chemical computations to evaluate global and local reactivity descriptors based on established structure–activity relationships (Cerda-Monje et al., 2014; Mendoza-Huizar and Rios-Reyes, 2011). Such descriptors include frontier molecular orbitals and Fukui functions, which describe molecular electronic structures and identify regions of highest electron density where oxidizing species attack.

This study is aimed at determining the effectiveness of electrochemical oxidation using graphite electrodes, for decolorization of disperse blue 1 dye (DBD) in aqueous solution. The effect of such variables as initial dye concentrations, electrolysis time, initial pH, supporting electrolyte concentration and temperature were assessed. Quantum chemical computations within the framework of the density functional theory (DFT) computations were used to predict the reactive sites for initiation of oxidative degradation on the DBD molecule.

2. Material and methods

2.1. Materials preparation

Disperse blue 1 dye (DBD) obtained from Aldrich, with dye content 30%, was used to prepare test solutions in the concentration range 25 – 145 mg/L. Sodium chloride (Sinopharm, China) was used as supporting electrolyte. Sulphuric acid and sodium hydroxide also obtained from Sinopharm, China were used for pH adjustment. All the other chemicals were analytical reagent grade and used without further purification.

2.2. Dye decolorization experiments

Electrochemical decolorization of DBD solutions was carried out in an electrolytic cell of 500 cm^3 capacity, with a magnetic stirrer. Both the anode and cathode were made of graphite plates of dimensions 100 x 30 x 2 mm and connected to a digital DC power supply (MCH-K305D). NaCl (0.1 M) was used as supporting electrolyte and added to the dye solution prior to electrolysis. The pH of the dye solution was adjusted by adding 1 M H_2SO_4 or 0.1 M NaOH as appropriate. For each experimental run, DBD was first mixed with the required amount of a sodium chloride and then introduced into the electrolysis cell. The test solution pH was adjusted as necessary. The electrodes were connected to the DC power supply and current density was set to the desired value (15 mA/cm^2). Exactly 2 ml of the samples were aspirated at 30 min intervals during the

electrolysis process, up to 180 min, and then sent for analysis. Experimental variables included initial DBD concentration (25 – 145 mg/L), solution pH (4, 7, 9), temperature (28, 50ºC). All experiments were performed in triplicate.

2.3. Analytical procedure

DBD concentrations were determined using an ultraviolet/visible (UV–Vis) spectrophotometer (LI-722) at maximum wavelength (λ_{max} = 615 nm) for dye solutions before and after electrolysis. The decolorization efficiency was calculated using (Eq. 1):

$$DE\% = \frac{C_0 - C_t}{C_0} \times 100 \qquad (5)$$

where, C_0 is the initial dye concentration (mg/L) and C_t the dye concentration (mg/L) after electrolysis for a time interval, t.

2.4. Quantum chemical computations

All theoretical computations were performed using the density functional theory (DFT) electronic structure programs DMol3 as contained in the Materials Studio 7.0 software (Biovia Scientific Innovation).

3. Results and discussion

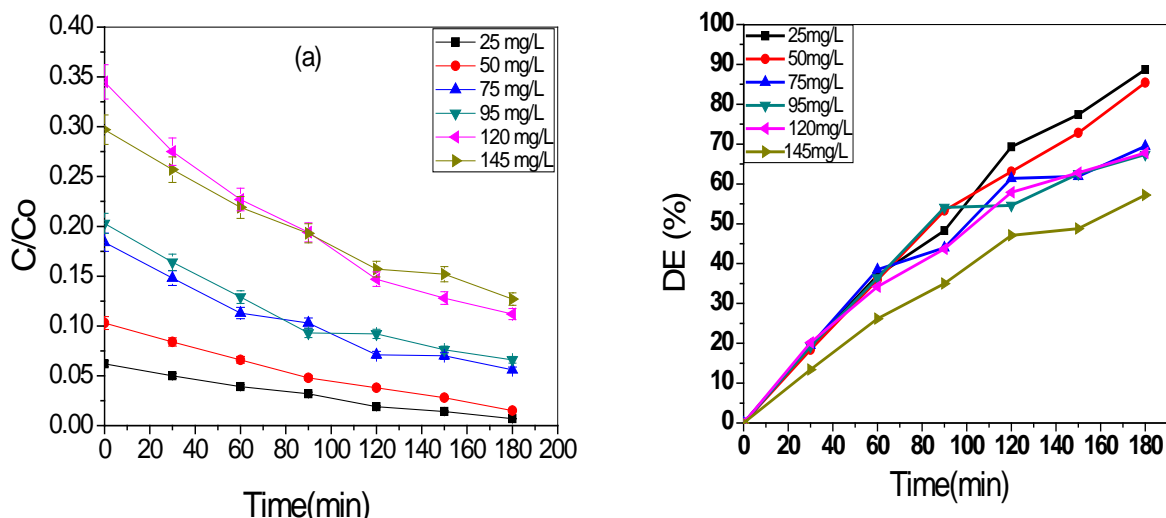### 3.1. Effect of initial concentration of DBD

The effect of the initial DBD concentration on the decolorization rate is shown in Fig. 1a, while the corresponding degradation efficiency values (DE%) shown in Fig. 1b. Increasing the dye concentration from 25 to 145 mg/L led to a decrease in the rate of electrochemical colour removal, causing the decolorization efficiency to drop from 88.7% to 67.8%. It has been suggested that high dye concentrations could lead to deposition of excess dye

on the surfaces of electrodes, which hinders the production of Cl⁻ ion thereby decreasing the decolorization efficiency (Asghar et al., 2015; Martınez-Huitle and Brillas, 2009; Rathinakumaran and Meyyappan, 2015; Yusuf et al., 2016). Moreover, dye molecules will tend to agglomerate at higher concentrations, forming clusters that will restrict migration rates towards the anode, with associated reduction in decolorization rates (El-Ashtoukhy and Amin, 2010).

3.2. Effect of Initial pH of DBD solution

Solution pH is a significant factor that affects the performance of electrochemical degradation processes, where the highest level of dye removal is attained at an optimal pH. The effect of initial pH of DBD solution on decolorization efficiency is illustrated in Fig. 2, for 25 mg/L and 120 mg/L concentrations of DBD. The pH of the dye solutions was adjusted with 1 M H_2SO_4 or 0.1 M NaOH. The plot shows decolorization efficiency to be more sensitive to pH changes at low DBD concentration, while remaining almost unchanged at higher concentrations. This effect should be related to the observed resistance of DBD to degradation at high concentrations.

Decolorization efficiency did not vary regularly with pH, but rather increased going from pH 4 (acidic) to pH 7 (neutral) and then decreased further going from pH 7 (neutral) to pH 9 (alkaline). Hence the optimal condition for DBD decolorization was achieved at pH 7. Baddouh et al. (2018) reported identical pH effects for the electrochemical decolorization of Rhodamine B dye in chloride-containing solution. Interpretation of the pH dependence of degradation processes can be quite challenging since pH affects several properties like the chemical states of solution species and solvent molecules, electrostatic interactions at the electrode/solution interphase, the type of active oxidizing species formed during the reaction, etc.

Fig. 1. Effect of initial DBD concentration on (a) decolorization rate (b) decolorization efficiency
(Current density = 15 mA/cm², Temperature (T) = 28 ºC, Voltage = 5 V, Electrolyte = 0.1 M NaCl)
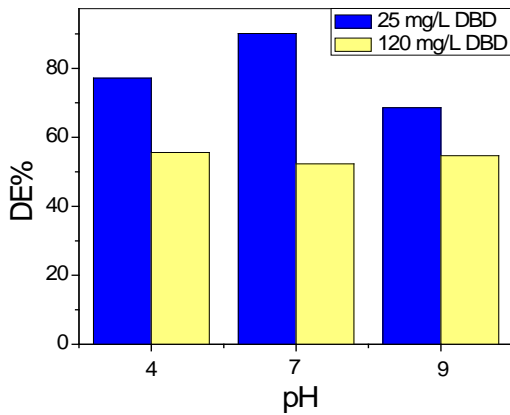
Fig. 2. Effect of solution pH on DBD decolorization efficiency (Current density = 15 mA/cm^2, T = 28 ^{o}C, Voltage = 5 V, Electrolyte = 0.1 M NaCl, Time (t) = 180 min)

For instance, the concentration of HOCl in solution (Eq. 3), as well as its ionization state (Eq. 4) is dependent on pH, with ClO$^-$ predominating beyond pH 7.5. The low oxidation potential of ClO$^-$ species when compared with Cl$_2$ and HOCl could thus be responsible for the considerably low decolorization efficiency at alkaline pH (Baddouh et al., 2018; Kariyajjanavar et al., 2011; Rajkumar et al., 2007).

3.3. Effect of temperature

Fig. 3 shows the temperature dependence of DBD decolorization efficiency as a function of electrolysis time. Experiments were undertaken at 28 and 50 ^{o}C using 25 mg/L (Fig. 3a) and 50 mg/L (Fig. 3b) solutions of DBD. The results show that decolorization efficiency increased with temperature, though the effect was much more pronounced at lower DBD concentration (25 mg/L), reaching 90% after 90 min and 96% after 180 min at 50 ^{o}C, compared to 60% and 80% respectively at 28 ^{o}C. Indeed, the influence of temperature on electro-oxidation of organics is neither consistent nor certain but varies according to the nature of the organic compound and the

environment. Hence, although temperature increase is ordinarily expected to lead to enhanced reaction rates, it has been observed in some cases to actually decrease electro-oxidation and decolorization rates. For instance, Ma et al. (2007) reported that increasing temperature beyond 25 ^{o}C decreased the rates of electro-catalytic oxidation and de-colorization of methyl orange in water containing NaCl as support electrolyte.

In the same manner, Panizza and Cerisola (2008) observed that the electrochemical oxidation of acid blue 22 by boron-doped diamond electrode was hindered at higher temperature. Rajkumar et al. (2007) also reported that an increase in temperature reduced the efficiency of electrochemical decolorization of reactive blue 19 in chloride medium. On the other hand, Tavares et al. (2012) reported that the electrochemical oxidation of methyl red using Ti/Ru$_{0.3}$TiO.7O$_2$ and Ti/Pt anodes was accelerated synchronously with increasing temperature from 25 – 60 ^{o}C. Increasing the temperature of electro-oxidation systems thus has dual effects; it increases the oxidation rate of organic contaminants by oxidizing species in solution and as well initiates the decomposition of the oxidizing species. In this regard, it has been suggested that temperature has minimal impact on electro-oxidation processes involving OH• radicals, whereas, generation of chlorine/hypochlorite is hindered by increase in temperature (Ma et al., 2007; Panizza and Cerisola, 2008). Relating the above scenarios to the present findings, it thus follows that at lower DBD concentrations the temperature enhancement of oxidation rate was the dominant effect, resulting in the observed pronounced increase in decolorization efficiency. At higher DBD concentration however, the second effect (decomposition of oxidizing species) kicks in, subduing the former effect and contracting the rate of increase in decolorization efficiency. The apparent activation energies (E_a) for the electrochemical degradation of DBD were evaluated from Arrhenius Eq. (6).

(a)

(b)
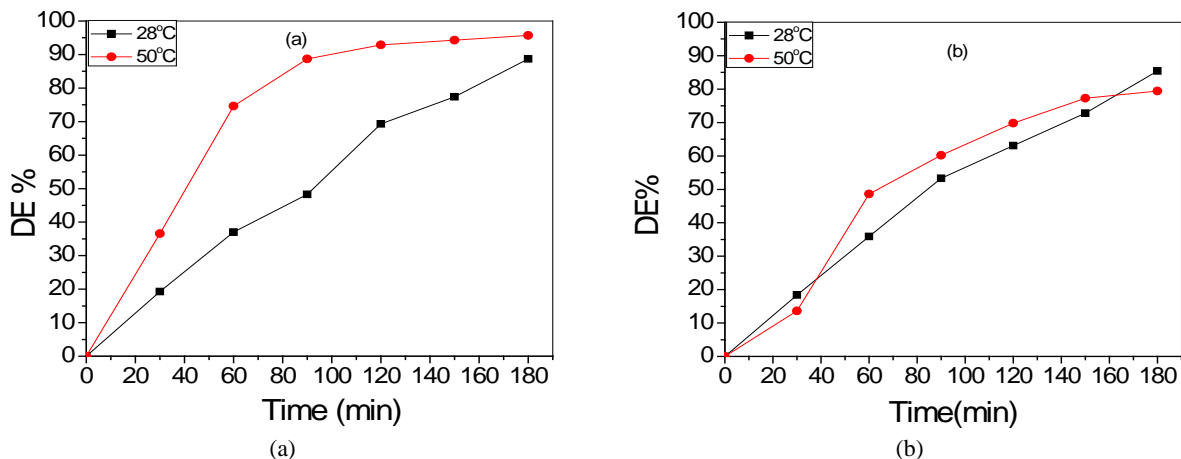
Fig. 3. Effect of temperature on decolorization efficiency for (a) 25 mg/L and (b) 50 mg/L DBD (Current = 15 mA/cm^2, pH = 7, Voltage = 5 V, Electrolyte = 0.1 M NaCl)

$$log\frac{\delta_2}{\delta_1} = \frac{E_a}{2.303R}\left(\frac{1}{T_1} - \frac{1}{T_2}\right) \qquad (6)$$

In Eq. (7), δ_1 and δ_2 are the DBD degradation rates at temperatures T_1 and T_2 respectively, while R is the universal gas constant. The δ values were obtained from the slopes of the C/C_0 vs. t plots. The obtained values of Ea were 11.9 kJ/mol and 30.5 kJ/mol for initial DBD concentrations of 25 mg/L and 50 mg/L respectively. The trend of degradation activation energies with DBD concentration is consistent with the experimental findings. The fact that the E_a value is lower at lower DBD concentration means that the degradation process would proceed more readily at lower than at higher DBD concentrations, as observed in this study.

3.4. Effect of current density

Current density is a measure of the number of electrons flowing between the anode and cathode and is thus a key parameter in controlling the rates of electrochemical processes. In order to study the effect of current density on the efficiency of electrochemical decolorization of DBD, five different values of current density ranging from 15 – 75 mA/cm² were tested, at a considerably high voltage of 25 V. Again, since it had earlier been established that the effectiveness of the decolorization process was significantly hindered at high DBD concentrations, experiments were carried out at low (15 mg/L) and high (75 mg/L) concentrations of DBD, in order to clarify whether higher current densities would overcome the limitations encountered at high DBD concentrations. The obtained results are presented in Fig. 4.

Fig. 4a shows the expected trend, wherein decolorization efficiency increased remarkably, even at shorter time intervals, with increasing current density, since high current density will enhance production of more of the highly oxidizing species like chlorine/hypochlorite (Baddouh et al., 2018;). Interestingly, the change of current density did not evoke any pronounced effects on decolorization efficiency at high DBD concentration (Fig. 4b). In other words, the accelerating effect associated with high current densities did not overcome the inhibiting effect posed by excess dye deposition on electrode surfaces at high DBD concentrations.

3.5. Effect of supporting electrolyte

Experiments were undertaken to assess the effect of different concentrations of two supporting electrolytes (KCl and Na₂SO₄) on the efficiency of decolorization of DBD at low and high concentrations. The obtained results after 60 mins of exposure are illustrated in Fig. 5 and Fig. 6 for KCl and Na₂SO₄ respectively.

Decolorization efficiency increased with concentration for both supporting electrolytes (KCl and Na₂SO₄). For KCl, this should be due essentially to an increase in the concentration and mobility of chloride ions and hypochlorite ions, which are the primary oxidizing species in solution. Similarly, high concentrations of Na₂SO₄, yields more of the powerfully oxidizing persulphate ions ($S_2O_8^{2-}$), which greatly enhanced DBD decolorization. Similar observations have been reported in the literature (Huimin et al., 2016; Kaur and Kaur, 2016; Rajkumar et al., 2007).

It is interesting that this electrolyte effect is pronounced at both low and high dye concentrations and as such is a veritable means for completely decolorizing dye solutions at high concentrations. Indeed, DBD decolorization efficiency approached 100% in the solution containing Na₂SO₄. It is noteworthy however that exceedingly high concentration of supporting electrolyte could adversely affect the colour removal process (Yang et al., 2016).

(a)

(b)
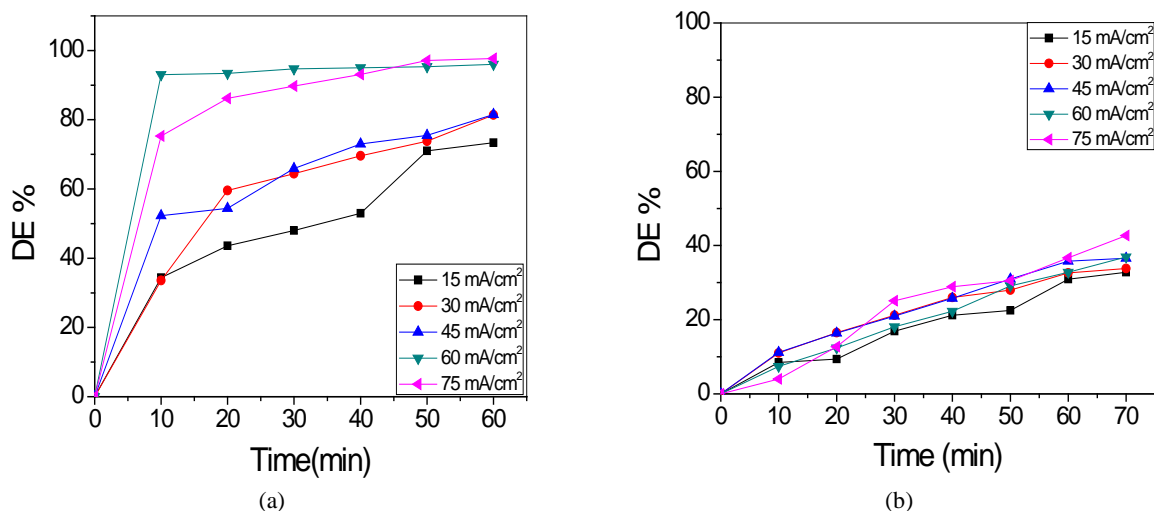
Fig. 4. Effect of current density on DBD decolorization efficiency for (a) 15 mg/L (b) 75 mg/L DBD
(Voltage = 25 V, T = 28 ºC, pH = 7, Electrolyte = 0.1 M NaCl)
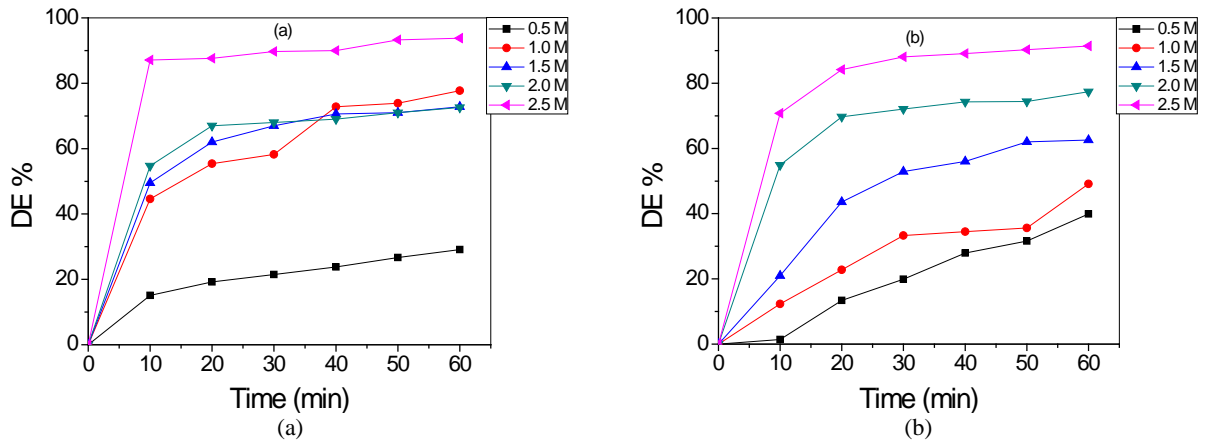
Fig. 5. Effect of KCl concentration on decolorization efficiency for (a) 15 mg/L (b) 75 mg/L DBD
(Current density = 75 mA/cm^2, T = 28 ^{o}C, pH = 7, Voltage = 25 V)
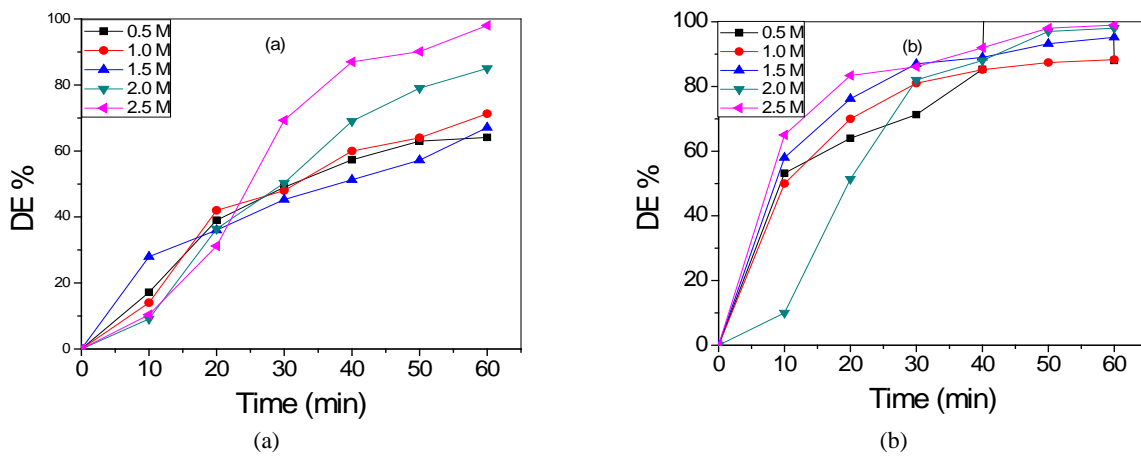
Fig. 6. Effect of Na$_2$SO$_4$ concentration on decolorization efficiency for (a) 15 mg/L (b) 75 mg/L DBD
(Current density = 75 mA/cm^2, T = 28 ^{o}C, pH = 7, Voltage = 25 V)

3.6. Energy consumption considerations

The electrical energy consumption associated with the electrochemical degradation of DBD can be estimated by calculating the electrical energy (kWh) used up in the process as follows (de Moura et al., 2016; Jović et al., 2013):

$$E(kWh) = \frac{P(W) \, x \, t(h)}{V_{sol}(dm^3)} \qquad (7)$$

where:

$$P(W) = I(A) \, x \, v(V) \qquad (8)$$

P is the electrical power of the electrochemical cell (in Watts); t is the electrolysis time (in hours); V_{sol} is volume of treated dye solution (in dm^3); I is the current (in Amperes) and v is voltage (in Volts).

Table 1 illustrates the relationship between applied current and electrical energy consumed for degradation of DBD at 25 V. As expected, the electrical energy consumed by the process increased steadily with increasing current and is of similar magnitude as the values for electrochemical degradation of a series of organic dyes, as reviewed by de Moura and co-workers (de Moura et al., 2016).

Table 1. Electrical energy input for degradation of DBD

Current (A/m^2)	*Voltage (V)*	*Time (h)*	*Energy consumption (kWh/m^3)*
150	25	1	7.5
300	25	1	15.0
450	25	1	22.5
600	25	1	30.0
750	25	1	37.5

The energy consumption values in Table 1 enables quantification of the cost of energy consumed per cubic meter of water contaminated by DBD, with respect to the average electricity tariff in Nigeria, which stands at about 36.6 NGN/kWh. This corresponds to 274.5 NGN (0.714 USD) – 1,372.5 NGN (3.57 USD) for the current range studied.

3.7. Decolorization initiation mechanism

In order to ascertain the mechanism of DBD decolorization, at least from a theoretical perspective, DFT computations were undertaken to model the local reactivity of the DBD molecule and hence identify the active sites through which the oxidative attack would be initiated. The DMol3 programme (Materials

Studio) was employed for the computations, using the Hirshfeld population analysis (Delley et al., 1990; Delley et al., 2000) and the Perdew–Wang (PW) local correlation, along with restricted spin polarization on the DND basis set. Prior to the computations, the molecular structure of DBD was initially geometrically optimized using the COMPASS force field with Smart minimization method by high-convergence criteria. Fig. 7 shows the optimized structure, highest occupied molecular orbital (HOMO), lowest unoccupied molecular orbital (LUMO) and Fukui functions of DBD from the computations. The HOMO regions, characterized by high electron density, are saturated around the p-phenyldiamine moieties, whereas the LUMO region appears spread-out over the molecule, though predominantly around the quinone moiety.

Table 2 shows some computed quantum chemical parameters for DBD, including the energies of the *HOMO (E_{HOMO})* and *LUMO (E_{LUMO})* as well as energy gap $\Delta E = E_{LUMO} - _{HOMO}$. Fukui indices (*FI*) were employed to assess reactive regions of the DBD molecule in terms of nucleophilic (F^+), electrophilic (F^-) and radical (F^0) attack. The obtained Fukui functions are presented in Table 3.

Table 2. Calculated quantum chemical properties for disperse blue 1 dye

Chemical Parameters	Values (eV)
E_{HOMO}	−4.47
E_{LUMO}	−3.40
Energy gap, $\Delta E_{gap} = (E_{LUMO} - E_{HOMO})$	1.07
Electrochemical potential, $\mu = -X$	−3.93
Ionization potential, I	4.47
Electron affinity, A	3.40
Electronegativity, X = (I+A)/2	3.93
Chemical hardness, η = (I-A)/2	0.27
Chemical softness, S =1/η	3.75
Electrophilicity, $\omega = \mu^2/ 2\eta$	28.98
$\Delta E_{Back donation}$ (−η/4)	−0.94

The HOMO regions, depicting the sites most prone to attack by electron seeking species, coincide with the locations of the electrophilic Fukui functions, which measure the propensity of the molecule to donate electrons, whereas the LUMO regions correspond with the F^+, which highlights the tendency of the molecule to receive electrons. Within the theoretical framework of the hard and soft acids and bases (HSAB) principle, it is possible to elucidate the electronic structures using basic molecular reactivity indicators (Cerda-Monje et al., 2014).

Accordingly, Table 2 provides some quantum-chemical descriptors connected to the molecular and electronic structure of DBD. A high value of E_{HOMO} describes the tendency of a species to give out electrons. Likewise, the lower the value of $\Delta E = E_{LUMO–HOMO}$, the lesser the energy needed to eject an electron from the outermost orbital. Chemical hardness (or softness) could be an important indicator of the propensity for electrophile/nucleophile interaction, since softness facilitates close contact

between the interacting species. The data presented in Table 3 suggest that the reactivity order for the various functional groups in the DBD molecule with respect to electrophilic attack is N15=N16=N17=N18>>C2=C3=C12=C13….>O19= O20. This means that the most reactive sites for attack by oxidizing (electrophilic) species are the amine functions in the p-phenyldiamine moieties. It is noteworthy that the propensity for electrophilic attack on the carbonyl functions of the quinone moiety is rather subdued.

Table 3. Calculated values of electrophilic, nucleophilic and radical Fukui indices for disperse blue 1 dye

No/ Atom	Electrophilic attack (F^-)	Nucleophilic attack (F^+)	Radical attack (F^0)
C (1)	0.032	0.025	0.029
C (2)	0.036	0.049	0.043
C (3)	0.036	0.049	0.043
C (4)	0.032	0.025	0.029
C (5)	0.021	0.016	0.018
C (6)	0.021	0.016	0.018
C (7)	0.010	0.048	0.029
C (8)	0.021	0.016	0.018
C (9)	0.021	0.016	0.018
C (10)	0.010	0.048	0.029
C (11)	0.032	0.025	0.029
C (12)	0.036	0.049	0.043
C (13)	0.036	0.049	0.043
C (14)	0.032	0.025	0.029
N (15)	0.067	0.035	0.051
N (16)	0.067	0.035	0.051
N (17)	0.067	0.035	0.051
N (18)	0.067	0.035	0.051
O (19)	0.029	0.067	0.048
O (20)	0.029	0.067	0.048
H (21)	0.025	0.030	0.027
H (22)	0.025	0.030	0.027
H (23)	0.025	0.030	0.027
H (24)	0.025	0.030	0.027
H (25)	0.029	0.022	0.025
H (26)	0.021	0.016	0.018
H (27)	0.029	0.022	0.025
H (28)	0.021	0.016	0.018
H (29)	0.021	0.016	0.018
H (30)	0.029	0.022	0.025
H (31)	0.021	0.016	0.018
H (32)	0.029	0.022	0.025

The reactivity order with respect to nucleophilic attack, which corresponds to *O19 = O20 > C2 = C3 = C12 = C13 > C7 = C10 > N15 = N16 = N17 = N18*, shows the most reactive sites to be on the quinone moiety. Interestingly, nucleophilic attack on the quinone moiety is consistent with the experimentally established decolorization mechanism of disperse blue 56, initiated by UV/sodium hypochlorite (Zeng et al., 2009). The values of the nucleophilic and electrophilic reactivity indices suggest that both attacks are equally probable. The radical reactivity order; N15 = N16 = N17 = N18 > O19 = O20 > C2 = C3 = C12 = C13 suggests possibility of attack mainly on the phenyldiamine and also on the quinone moiety.
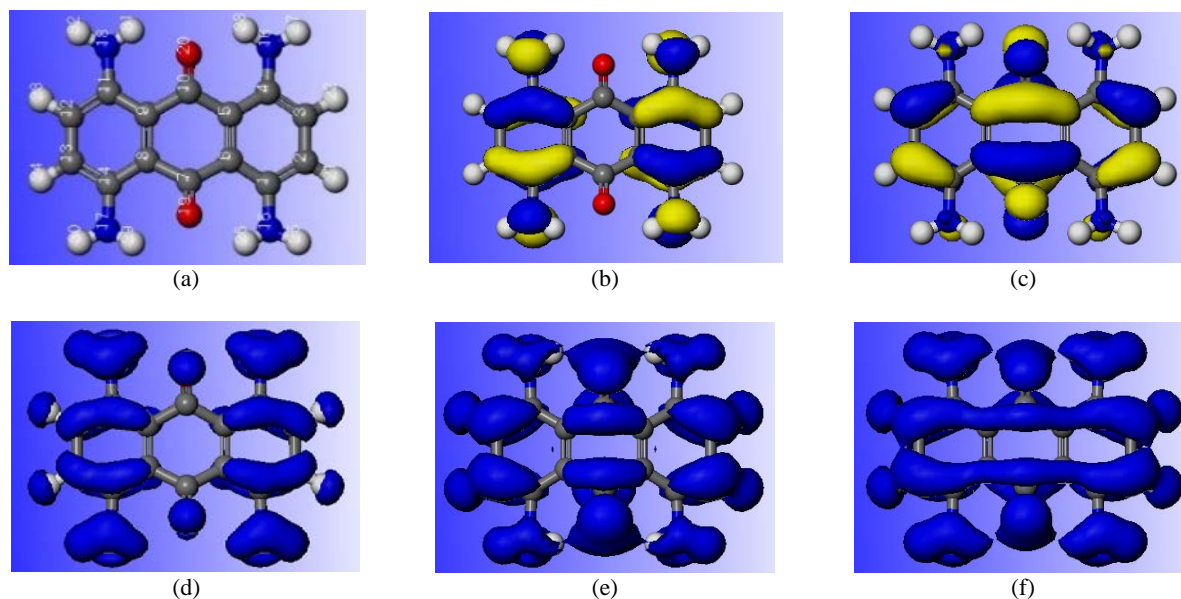
Fig. 7. Electronic properties of disperse blue 1 dye; (a) optimized structure, (b) HOMO, (c) LUMO, (d) Fukui F⁻,
(e) Fukui F⁺, (f) Fukui F

The values of all the computed quantum chemical descriptors suggest that the reactive sites for oxidative decolorization of DBD are located primarily on the amine functions in the p-phenyldiamine moieties.

4. Conclusions

Electrochemical decolorization of disperse blue dye (DBD) in aqueous solution using graphite electrodes was achieved in this study. The decolorization rate was hindered at high DBD concentrations, with correspondingly low decolorization efficiencies. Changes in solution pH influenced DBD decolorization, with the highest effect obtained at neutral pH. Decolorization efficiency was more sensitive to pH changes at low DBD concentration and almost unchanged at higher concentrations

Increasing the system temperature enhanced DBD oxidation rate and hence decolorization efficiency, particularly at lower DBD concentrations, a trend that was justified by lower degradation activation energies at low dye concentrations.

In the same vein, decolorization efficiency increased remarkably with current density at low DBD concentrations, even at shorter time intervals, but had negligible effect at high DBD concentrations. Interestingly, decolorization efficiency increased with concentration of both supporting electrolytes (KCl and Na_2SO_4), at both low and high DBD concentrations and as such is a veritable means for completely decolorizing dye solutions at high concentrations. Quantum chemical computations revealed the reactivity order for the various functional groups in the DBD molecule with respect to electrophilic attack to be N15 = N16 = N17 = N18 >> C2 = C3 = C12 = C13…. > O19 = O20. This indicates that oxidative

decolorization of DBD is initiated at the amine functions in the p-phenyldiamine function.

References

Abd El-Kader Sh.F., El-Chaghaby G.A., Khalafalla G.M., Refae R.I., Elshishtawy H.M., (2019), A novel microbial consortium from sheep compost for decolorization and degradation of Congo red, *Global Journal of Environmental Science and Management*, **5**, 61-70.

Alves S.A., Ferreira T.C.R., Migliorini F.L., Baldan M.R., Ferreira N.G., Lanza M.R.V., (2013), Electrochemical decolorization of the insecticide methyl parathion using a boron-doped diamond film anode, *Journal of Electroanalytical Chemistry*, **702**, 1-7.

An H., Cui H., Zhan G.W., Zhai J., Qian Y., Xie X., Li Q., (2012), Fabrication and electrochemical treatment application of a microstructured TiO₂-NTs/Sb–SnO₂/PbO₂ anode in the decolorization of C.I. Reactive Blue 194 (RB 194), *Chemical Engineering Journal*, **209**, 86-93.

Asghar H.M.A., Ahmad T., Hussain S.N., Sattar H., (2015), Electrochemical oxidation of methylene blue in aqueous solution, *International Journal Chemical Engineering Application*, **6**, 352-356.

Awad H.S., Galwa N.A., (2005), Electrochemical decolorization of acid blue and basic brown dyes on Pb/PbO₂ electrode in the presence of different conductive electrolyte and effect of various operating factors, *Chemosphere*, **61**, 1327-1335.

Baddouh A., Bessegato G.G., Rguiti M.M., El Ibrahimi B., Bazzi L., Hilali M., Zanoni M.V.B., (2018), Electrochemical decolorization of rhodamine b dye:

Influence of anode material, chloride concentration and current density, *Journal of Environmental Chemical Engineering*, **6**, 2041-2047.

Basha C.A., Sendhil J., Selvakumar K.V., Muniswaran P.K.A., Lee C.W., (2012), Electrochemical decolorization of textile dyeing industry effluent in batch and flow reactor systems, *Desalination*, **285**, 188-197.

Cerda-Monje A., Bal-Toledo R.O., Cardenas C., Fuentealba P., Contreras R., (2014), Regional electrophilic and nucleophilic Fukui functions efficiently highlight the Lewis acidic/basic regions in ionic liquids, *Journal of Physical Chemistry B*, **118**, 3696-3701.

de Moura D.C., Quiroz M.A., Da Silva D.R., Salazar R., Martinez-Huitle C.A., (2016), Electrochemical degradation of Acid Blue 113 dye using TiO_2-nanotubes decorated with PbO_2 as anode, *Environmental Nanotechnology, Monitoring and Management*, **5**, 13-20.

Delley B.J., (1990), An all-electron numerical method for solving the local density functional for polyatomic molecules, *Journal of Chemical Physics*, **92**, 508-517.

Delley B.J., (2000), From molecules to solids with the Dmol3 approach, *Journal of Chemical Physics*, **113**, 7756-7764.

El-Ashtoukhy E-S.Z., Mobarak A.A., Fouad Y.O., (2016), Decolourization of reactive blue 19 dye effluents by electrocoagulation in a batch recycle new electrochemical reactor, *International Journal of Electrochemical Science*, **11**, 1883-1897.

El-Ashtoukhy E-S.Z., Amin N.K., (2010), Removal of acid green dye 50 from wastewater by anodic oxidation and electrocoagulation-A comparative study, *Journal of Hazardous Material*, **179**, 113-119.

El-Sayed G.O., Awad M.S., Ayad Z.A., (2014), Electrochemical decolorization of maxilon red GRL textile dye, *International Research Journal of Pure and Applied Chemistry*, **4**, 402-416.

Eren B., Keskin C., Ozdemir A., (2020), Photocatalytic degradation of disperse blue 56 by cu-ti-pilcs and fe-ti-pilcs, *Environmental Engineering and Management Journal*, **19**, 1261-1268.

Forgacs E., Cserhati T., Oros G., (2004), Removal of synthetic dyes from wastewaters: a review, *Environment International*, **30**, 953-971.

Gholami M., Davoudi M., Farzadkia M., Esrafili A., Dolati A., (2018), Electrochemical degradation of clindamycin by anodic oxidation on sno2-sb coated titanium anodes, *Environmental Engineering and Management Journal*, **17**, 343-355.

Gupta V.K., Khamparia S., Tyagi I., Jaspal D., Malviya A., (2015), Decolorization of mixture of dyes: A critical review, *Global Journal of Environmental Science and Management*, **1**, 71-94.

Huimin Y., Jintao L., Li Z., Zhenhai L., (2016), Electrochemical oxidation degradation of methyl orange wastewater by Nb/PbO_2 electrode, *International Journal of Electrochemical Science*, **11**, 1121-1134.

Jawad N.J., Najim S.T., (2018), Removal of methylene blue by direct electrochemical oxidation method using a graphite anode, *Material Science Engineering*, **454**, 012023, http://doi.org/10.1088/1757-899X/454/1/012023.

Jan F., Ullah R., Shah U., Saleem M., Ullah N., (2020), Band gap tuning of zinc oxide nanoparticles by the addition of (1-4%) strontium. synthesis, characterization of the catalyst and its use for the photocatalytic degradation of acid violet-17 dye in aqueous solution, *Environmental Engineering and Management Journal*, **19**, 2039-2048.

Jović M., Stanković D., Manojlović D., Anđelković I., Milić A., Dojčinović B., Roglić G., (2013), Study of the Electrochemical Oxidation of Reactive Textile Dyes Using Platinum Electrode, *International Journal of Electrochemical Science*, **8**, 168-183.

Kariyajjanavar P., Jogttappa N., Nayaka Y.A., (2011), Studies on decolorization of reactive textile dyes solution by electrochemical method, *Journal of Hazardous Material*, **190**, 952-961.

Kariyajjanavar P., Narayana J., Nayaka Y.A., (2011), Decolorization of textile wastewater by electrochemical method, *Hydrology: Current Research*, **2**, 110, http://dx.doi.org/10.4172/2157-7587.1000110.

Kaur R., Kaur H., (2016), Electrochemical decolorization of congo red from aqueous solution: Role of graphite anode as electrode material, *Portugaliae Electrochimica Acta*, **34**, 185-196.

Khalik W., Ong S., Ho L., Wong Y., Yusoff N., Ridwan F., (2018), Comparison on solar photocatalytic degradation of orange g and new coccine using zinc oxide as catalyst, *Environmental Engineering and Management Journal*, **17**, 391-398.

Kolekar Y.M., Pawar S.P., Gawai K.R., Lokhande P.D., Shouche Y.S., Kodam K.M., (2008), Decolorization and degradation of disperse blue 79 and acid orange 10, by *Bacillus fusiformis KMK5* isolated from the textile dye contaminated soil, *Journal of Biotechnologyech*, **99**, 8999-9003.

Koparal A.S., Yavuz Y., Gürel C., Oğütveren U.B., (2007), Electrochemical decolorization and toxicity reduction of C.I. basic red 29 solution and textile wastewater by using diamond anode, *Journal of Hazardous Material*, **145**, 100-108.

Lopes A., Martins S., Morão A., Magrinho M., Gonçalves I., (2004), Decolorization of a textile dye C. I. direct red 80 by electrochemical processes, *Portugaliae Electrochimica Acta*, **22**, 279-294.

Ma H., Wang B., Luo X., (2007), Studies on decolorization of methyl orange wastewater by combined electrochemical process, *Journal of Hazardous Material*, **149**, 492-498.

Martınez-Huitle C.A., Brillas E., (2009), Decontamination of wastewaters containing synthetic organic dyes by electrochemical methods: A general review, *Appiled Catalyst B: Environment*, **87**, 105-145.

Mendoza-Huizar L.H., Rios-Reyes C.H., (2011), Chemical reactivity of atrazine employing the Fukui function, *Journal of Mexican Chemical Society*, **55**, 142-147.

Pan H., Xu X., Wen Z., Kang Y., Wang X., Ren Y., Huang D., (2017), Decolorization pathways of anthraquinone dye disperse blue 2BLN by *Aspergillus sp. XJ-2 CGMCC12963*, *Bioengineered*, **8**, 630-641.

Panizza M., Cerisola G., (2008), Removal of colour and COD from wastewater containing acid blue 22 by electrochemical oxidation, *Journal of Hazardous Materials*, **153**, 83-88.

Pearce C.I., Lloyd J.R., Guthrie J.T., (2003), The removal of color from textile wastewater using whole bacterial cells: a review, *Dyes and Pigments*, **58**, 179-196.

Rahimi B., Ebrahimi A., Mansouri N., Hosseini N., (2019), Photodegradation process for the removal of acid orange 10 using titanium dioxide and bismuth vanadate from aqueous solution, *Global Journal of Environmental Science and Management*, **5**, 43-60.

Rahimi S, Singh MP, Gupta J. (2020), Adverse effects of textile dyes on antioxidant enzymes and cholinesterase activities in Drosophila melanogaster (Oregon R+), *Drug and Chemical Toxicology*, **24**, doi: 10.1080/01480545.2020.1809671.

Rajkumar D., Song B.J., Kim J.G., (2007), Electrochemical decolorization of reactive blue 19 in chloride medium for the treatment of textile dyeing wastewater with identification of intermediate compounds, *Dyes and Pigments*, **72**, 1-7.

Rathinakumaran K., Meyyappan R.M., (2015), Electrochemical decolorization of dye effluents using mixed oxide coated DSA electrode-A kinetic study, *International Journal of Chemical Science*, **13**, 1401-1409.

Routoula E., Patwardhan S.V., (2020), Degradation of Anthraquinone Dyes from Effluents: A review focusing on enzymatic dye degradation with industrial potential, *Journal of Environmental Science and Technology*, **54**, 647-664.

Saquib M., Tariq M.A., Haque M.M., Muneer M., (2008), Photocatalytic decolorization of disperse blue 1 using $UV/TiO_2/H_2O_2$ process, *Journal of Environmental and Management*, **88**, 300-306.

Stergiopoulos D., Dermentzis K., Giannakoudakis P., Sotiropoulos S., (2014), Electrochemical decolorization and removal of indigo carmine textile dye from wastewater, *Global NEST Journal*, **16**, 499-506.

Tavares M.G., da Silva L.V.A., Sales Solano A.M., Tonholo J., Martínez-Huitle C.A., Zanta C.L.P.S., (2012), Electrochemical oxidation of Methyl Red using Ti/Ru0.3Ti0.7O2 and Ti/Pt anodes, *Chemical Engineering Journal*, **204-206**, 141-150.

Yong K., Zhi-Liang W., Yu W., Jia Y., Zhi-Dong C., (2011), Decolorization of methyl orange in artificial wastewater through electrochemical oxidation using exfoliated graphite electrode, *New Carbon Material*, **26**, 459-464.

Yusuf H.A., Redha Z.M., Baldock S.J., Fielden P.R., Goddard N.J., (2016), An analytical study of the electrochemical decolorization of methyl orange using a novel polymer disk electrode, *Microelectronic Engineering*, **149**, 31-36.

Zeng Q.F., Fu J., Shi Y.T., Zhu H.L., (2009), Decolorization of C.I. disperse blue 56 by ultraviolet radiation/sodium hypochlorite, *Ozone Science Engineering*, **31**, 37-44.